Effect of Strain on the Photoisomerization and Stability of a Congested Azobenzenophane: A Combined Experimental and Computational Study

Elisa Bassotti,[†] Paola Carbone,[†] Alberto Credi,[*,†] Marco Di Stefano,[†] Stefano Masiero,[‡,§] Fabrizia Negri,[*,†,§] Giorgio Orlandi,[†,§] and Gian Piero Spada[‡,§]

Dipartimento di Chimica 'G. Ciamician', Università di Bologna, Via F. Selmi, 2, 40126 Bologna, Italy, Dipartimento di Chimica Organica "A. Mangini", Università di Bologna, Via San Giacomo 11, 40126 Bologna, Italy, and INSTM, UdR Bologna, Italy

Received: April 20, 2006; In Final Form: September 12, 2006

The stability and trans−cis photoisomerization properties of a macrocycle constituted of two *para*-aminoazobenzene units connected by two methylene bridges have been investigated by a combination of experimental and computational techniques. Irradiation at 365 nm leads to a photostationary state in which only 50% of the azobenzene units have isomerized, in contrast with the behavior of *para*-aminoazobenzene, whose photoconversion is larger than 80%. In the case of the macrocycle, a faster cis → trans thermal back-reaction is observed. To assist the interpretation of the experimental results, molecular mechanics and quantum chemical calculations have been carried out. Of the possible conformers, the most stable trans−trans geometric isomer has been identified along with the more plausible trans−cis and cis−cis isomers. Ground-state energy barriers along the NN torsional coordinates were also computed, along with excitation energies and intensities for the species that can contribute to the photostationary state. The calculations point to a sequential photoisomerization mechanism and support a predominance of the trans−cis photoproduct with minor contributions from the cis−cis species. The thermal and photochemical reactivity of the examined macrocycle is compared to that of previously investigated azobenzenophanes and explained in terms of strain and substituent effects both concurring to favor the thermal cis → trans back-reaction.

1. Introduction

Azobenzene is a typical molecular switch whose reversible cis−trans isomerization is associated with remarkable changes in the structure and chemical properties.[1] Introduction of the photoresponsive azobenzene unit in functional molecules or organized molecular systems enables the switch, induced by light, of the functions of these materials.[2−7] In macrocyclic compounds including two azobenzene units the light-induced isomerization of one photoresponsive unit and the backward thermal isomerization are usually affected by the size and conformation of the remaining part of the ring, owing to the ring strain.[4,5] A first example in this sense is represented by the work of Rau on the photochemical and thermal isomerization reactions of a [3.3](4,4′)-azobenzenophane, where the azobenzene units are connected by $-CH_2-S-CH_2-$ bridges.[8] This compound was found to photoisomerize reversibly by successive isomerization of the two units with a photoconversion close to 95%, but the thermal cis → trans isomerization was shown to be 1000 times faster at room temperature when the other azobenzene unit is in the trans (**t**) form than when it is in the cis (**c**) form.[8] More recent studies have shown that the shorter the length of the bridges at the para positions of the azobenzenophane, the more significant is the effect of the second azobenzene unit on the isomerization rate of the first, owing to the strain induced by the cis form. In this regard Tamaoki showed that the [2.2](4,4′)-azobenzenophane in which two azobenzenes are connected by $-CH_2-CH_2-$ bridges[9,10] isomerizes thermally from the trans−cis (**tc**) to the trans−trans (**tt**) form in only 22 s. Notice that the compound photoisomerizes readily upon irradiation at 366 nm and a photostationary state (PSS) in which 88% of the **tt** form has isomerized is obtained. Tauer and co-workers synthesized a [2.2](2,2′)-azobenzenophane (**1**, Chart 1) with bridges formed by two atoms ($-CH_2-CH_2-$) bound at the ortho positions of the photoresponsive units.[11] Both **tc** and cis−cis (**cc**) forms were obtained upon irradiation, but in contrast with the [3.3](4,4′)- and [2.2](4,4′)-azobenzenophanes, both **tc** and **cc** forms were found to thermally isomerize slowly and the lifetime of the **tc** form was found to be longer than that of the **cc** form.

More recently, an azobenzenophane with linkers consisting of a single atom at the meta positions has been reported.[12,13] The [1.1](3,3′)-azobenzenophane **2** (Chart 1) showed stepwise photoisomerization in solution, and the lifetime of the **cc** isomer was found to be three times longer than that of the **tc** isomer.

These previous studies show that the photochemical and thermal isomerization properties of azobenzenophanes along with the stability of the isomeric forms are affected by the position of the linkers and by their chain length. With this work we add a new term to the series of investigated cyclic azo compounds by considering the azobenzenophane **4** (Chart 1) formed by two units of *para*-aminoazobenzene (**3**) linked by one-atom bridges. Each aromatic ring in the two photoresponsive units of the macrocycle is bound to the one atom linker in a different position, namely, the ortho position for the aminobenzene ring and the meta position for the unsubstituted phenyl. To the best of our knowledge this is the first example of an azobenzenophane with one-atom linkers binding the two pho-

* To whom correspondence should be addressed. A.C.: E-mail alberto.credi@unibo.it. F.N.: E-mail fabrizia.negri@unibo.it.
[†] Dipartimento di Chimica 'G. Ciamician', Università di Bologna.
[‡] Dipartimento di Chimica Organica "A. Mangini", Università di Bologna.
[§] INSTM.

10.1021/jp062428b CCC: $33.50
Published on Web 10/26/2006

CHART 1: Structural Formula of [2.2](2,2′)-Azobenzenophane (1), [1.1](3,3′)-Azobenzenophane (2), *para*-Aminoazobenzene (3), and Azobenzenophane (4) Investigated in This Work

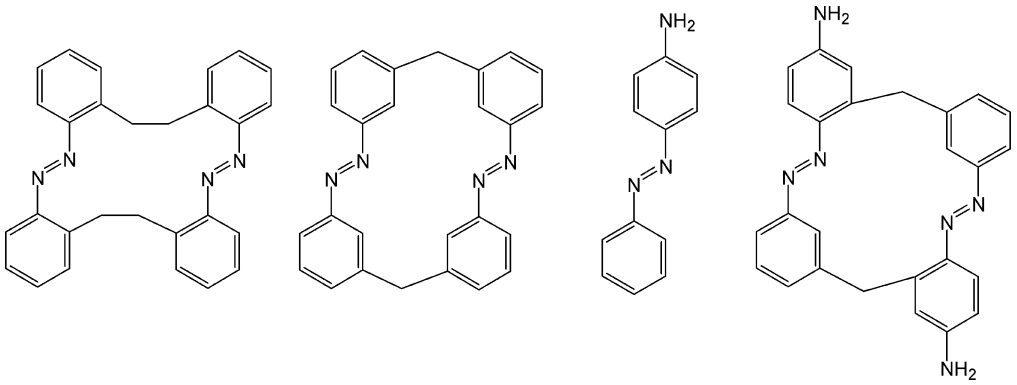

TABLE 1: Absorption, Photoisomerization, and Thermal Isomerization Data

	absorption,[a] λ_{max}, nm (ϵ, M^{-1} cm^{-1})	**t** → **c** photoreaction,[b] F	%(**c**) PSS[c]	**c** → **t** thermal back reaction, k, s^{-1}
azobenzene				
t	316(29 000)−442(770)	0.14	95	4.3×10^{-6}
compound **3**				
t	382(28 000)[d]	0.15	80	1.7×10^{-4}
c	343(8700)−447(3200)			
compound **4**				
tt	392(32 400)	0.11	50	3.6×10^{-4}
PSS	388			
c units[e]	347(3800)−466(2700)			

[a] Air-equilibrated acetonitrile solution and ambient temperature (295 K). [b] Irradiation at 365 nm. [c] Fraction of **c** azobenzene units at the photostationary state (PSS). [d] n−π* band overlapped with the π−π* band. [e] Absorption maxima attributed to **c** units in the photoproduct of **4**.

toresponsive units at two different positions (meta and ortho). The effect of strain on the photoisomerization properties and stability of the various configurational and conformational isomers of **4** is explored by a combination of experimental and computational investigations, and a comparison with the properties of model compound **3** is presented.

2. Methods

2.1. Experimental Section. Compound **4** was prepared according to ref 14. Compound **3** is a commercial product (from Aldrich). The absorption spectra were recorded with a Perkin-Elmer λ40 spectrophotometer on air-equilibrated acetonitrile (Merck Uvasol) solutions at room temperature (295 K) with concentrations ranging from 1×10^{-5} to 1×10^{-4} mol L^{-1}, contained in 1-cm quartz cells. Experimental errors: wavelengths, ±1 nm; molar absorption coefficients, ±5%.

Photochemical reactions were performed on the same solutions, thoroughly stirred, using the 365-nm line of a Hanau Q 400 medium-pressure Hg lamp (150 W), isolated by means of an interference filter. The number of incident photons, determined by ferrioxalate actinometry[15] in its microversion,[16] was on the order of 10^{-7} *Nhν*/min in the irradiated volume (3 mL). The trans → cis quantum yields were determined from the disappearance of the π−π* absorption band of the trans form at low conversion percentages (<10%) to minimize the error caused by the occurrence of the back cis → trans photochemical and thermally activated isomerization. To the same purpose, the Φ values reported in Table 1 were obtained from determination of the quantum yield at successive irradiation times t and extrapolation for $t_0 = 0$. The fraction of light transmitted at the irradiation wavelength was taken into account in the calculation of the yields.[17] Owing to the fast thermal back-isomerization it was not possible to determine the composition of the photostationary state of **3** and **4** by HPLC analysis (and for **4** by ^{1}H NMR); hence, the absorption spectrum of the photoproduct (cis isomer), and consequently the composition of the PSS, was evaluated from a calibrated subtraction of the spectrum of the residual trans isomer from the absorption spectrum at the photostationary state after a qualitative optimization of the calculated curve. The thermal cis → trans isomerization was studied at room temperature (295 K) by monitoring the absorption spectral changes versus time for 5.0 $\times 10^{-5}$ mol L^{-1} solutions previously subjected to exhaustive irradiation at 365 nm. The concentration values of the cis form at various times were calculated by means of eq 1

$$[\mathbf{c}]_t = [\mathbf{t}]_0 - \frac{A_\lambda}{d(\epsilon_{t,\lambda} - \epsilon_{c,\lambda})} \quad (1)$$

where $[\mathbf{c}]_t$ is the concentration of the cis form at time t, $[\mathbf{t}]_0$ is the initial concentration of the solution containing the trans form, A_λ is the absorbance value at wavelength λ, d is the optical path length (1 cm), and $\epsilon_{\mathbf{t},\lambda}$ and $\epsilon_{\mathbf{c},\lambda}$ are the molar absorption coefficients at wavelength λ of the trans and cis forms, respectively. The monitored wavelength was that of the absorption maximum of the trans form, namely, 382 nm for **3** and 387 nm for **4**. The so-obtained $[\mathbf{c}]_t$ data were satisfactorily fitted according to a first-order rate equation. The experimental error on the quantum yield and rate constant values were estimated to be 10%.

2.2. Computations. The ground-state structure of **4** was initially optimized with molecular mechanics calculations using the MM3 force field.[18] A partial conformational search was carried out using the general conformational search algorithm implemented in the Tinker[19] software package. The five lowest frequency normal modes were used to scan the potential-energy surface, and the energy threshold was set to 100 kcal/mol. The equilibrium structures of the three isomers [**tt**, **tc**, and **cc**] of the cyclic azo compound **4** obtained from the MM3 calculations and those of the two isomers [**t** and **c**] of compound **3** were subsequently optimized with quantum chemical calculations at the HF/3-21G level of theory, and the nature of the stationary points was assessed by computing the corresponding vibrational frequencies. Estimates of ground-state barriers were obtained

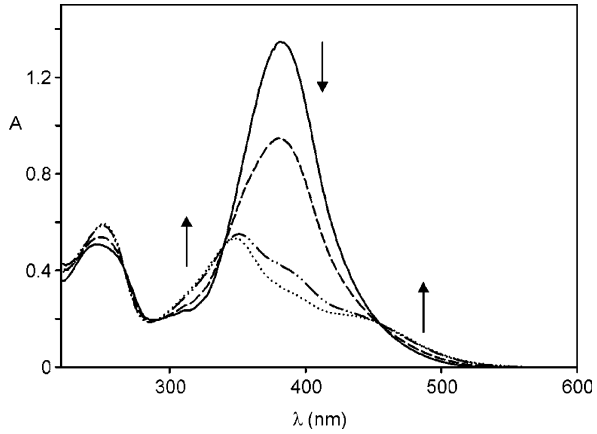

Figure 1. Absorption spectrum of a 5.0×10^{-5} mol L^{-1} acetonitrile solution of **3** at room temperature (full line), and absorption spectral changes on 365 nm irradiation of the same solution for 1.5 (dashed line), 4 (dashed−dotted line), and 5 (dotted line) min. The latter spectrum corresponds to the photostationary state.

by performing relaxed potential energy surface (PES) scans along the NN torsional coordinate with a step size of 1.0°. The HF/3-21G equilibrium geometries were employed to calculate electronic excitation energies with the ZINDO/S semiempirical Hamiltonian[20] combined with configuration interaction singles (CIS) calculations. To obtain a qualitative picture of the $\pi-\pi^*$ excited-state geometry relaxation, selected excited-state geometry optimizations were performed at CIS/3-21G level of theory. Ab initio CIS calculations with moderate basis sets are known to overestimate excitation energies but provide a reliable description of the geometry relaxation for excited states dominated by single excitations. Given the large dimension of the molecules investigated, the orbital space was restricted to 10×10. All calculations were carried out with the Gaussian 03[21] suite of programs. The visual program Molekel[22] was employed to plot optimized molecular structures.

3. Results

3.1. Photoisomerization Reactions of 3 and 4. The absorption spectrum of the **t** isomer of **3** in acetonitrile solution is shown in Figure 1. The spectroscopic data are collected in Table 1. In contrast with azobenzene, **3** shows a one-band pattern, which includes the $\pi-\pi^*$ and $n-\pi^*$ absorption features, owing to the reduced energy gap between the two excited states.[23] The absorption maximum is observed at 382 nm, the remarkable shift to lower energies compared to azobenzene being induced by the para amino group.[23]

The **t** → **c** photoisomerization quantum yield and the composition of the PSS for irradiation at 365 nm are also reported in Table 1. Figure 1 shows the absorption changes observed upon irradiation of the **t** isomer of **3** at 365 nm. Such changes are consistent with the **t** → **c** isomerization of the azobenzene unit: the band with maximum at 382 nm decreases and is replaced by two bands with maxima at 447 and 352 nm. The photoisomerization quantum yield of the **t** form of **3** is close to that of *trans*-azobenzene; conversely, the thermal back reaction of cis-**3** is much faster than that of *cis*-azobenzene[24] as expected because of the presence of the *para*-amino substituent.[25] In our conditions the **t** form of **3** is quantitatively regenerated in less than 2 h, starting from the PSS. Indeed, the activation energy of the **c** → **t** thermal conversion is ca. 23 kcal/mol for azobenzene and its derivatives, except for those containing substituents which cause intramolecular changes, such as the production of tautomeric species and thereby lowering the energy of the activated intermediate.

TABLE 2: MM3 and HF/3-21G Relative Energies for Compound 3 and Selected Conformers of the Three Geometrical Isomers of 4, and ZINDO/S Vertical Excitation Energies Computed for the Lowest $\pi-\pi^*$ Transitions

isomer	ΔE, kcal/mol MM3	ΔE, kcal/mol HF/3-21G	$\pi\pi^*$ states, nm[a] (f [b])
compound **3**			
t		0.0	366(0.97)
c		20.1	337(0.38)
compound **4**			
tt1(uu)	0.0	0.0	392(0.00)−366(1.68)
tt1(ud)	4.5	5.8	364(0.00)−348(1.50)
tt2(uu)	6.0	7.8	383(0.12)−362(1.50)
tt2(ud)	8.0		
tt3(uu)	12.6	16.0	369(0.00)−360(1.54)
tt3(ud)	17.4		
tc1	18.5	25.0	361(0.63)−332(0.27)
tc2	17.9	20.6	372(0.56)−347(0.50)
cc1	29.0	40.7	351(0.21)−341(0.21)
cc2	32.2	41.2	364(0.02)−354(0.18)

[a] Vertical excitation energy for the lowest $\pi-\pi^*$ transitions predicted from ZINDO/S calculations. [b] Oscillator strength.

The presence of a set of clean isosbestic points at 267, 291, 340, and 455 nm, which are maintained throughout the irradiation, is consistent with the existence of two species, namely, the **c** and **t** forms of **3**. Since the PSS is reached within 5 min of irradiation, it can be estimated that its composition is not largely affected by the thermal back reaction. However, attempts to determine the amount of **c** isomer present at the PSS failed. HPLC analysis of the irradiated solution showed the presence of the **t** form only: evidently, in the conditions and on the time scale of the HPLC experiment, the **c** form reverts thermally to the **t** one. Therefore, the absorption spectrum of the **c** form and the composition of the PSS were evaluated by subtracting the spectrum of the **t** isomer from that of the PSS (see Experimental Section). The absorption spectrum of *cis*-**3** shows two bands in the near-UV region, centered at 343 and 447 nm (Table 1).

The experimental absorption spectra of the two isomers of **3** can be compared with the ZINDO/S vertical excitation energies computed at the HF/3-21G-optimized ground-state geometries and collected in Table 2. The lowest energy $\pi-\pi^*$ transition of the **t** form is predicted at 366 nm, in good agreement with the experimental data. The observed $\pi-\pi^*$ transition blue shifts to 343 nm for the **c** isomer of **3**, and similarly the computed excitation energy increases to 337 nm. Thus, the spectral changes upon **t** → **c** isomerization are correctly reproduced by the ZINDO/S calculations, except for a slight energy overestimate. The same trend can be expected for the azobenzenophane **4** composed by the two photoresponsive units **3**.

The solid line in Figure 2 shows the absorption spectrum of the **tt** isomer of **4** in acetonitrile. The spectrum shows a peak centered at 392 nm, only slightly red shifted compared to compound **3**. Figure 2 shows also the absorption changes observed upon irradiation at 365 nm. The intensity of the 392 nm band decreases as expected for a **t** → **c** isomerization of the azobenzene units, the position of the maximum shifts slightly to higher energies (ca. 388 nm), and a PSS is obtained after irradiation for 25 min. Similarly to compound **3**, owing to the fast thermal back reaction, the composition of the PSS could not be measured by HPLC analysis.[26] Although, in principle, the three isomeric forms (**tt**, **tc**, and **cc**) of **4** can contribute to the PSS, inspection of Figure 2 shows that the intensity of the

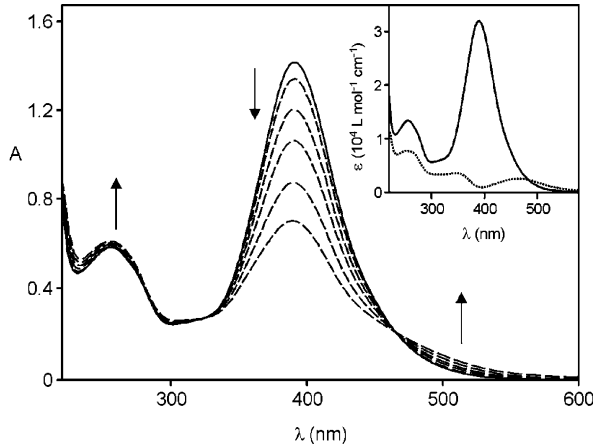

Figure 2. Absorption spectrum of a 4.4×10^{-5} mol L^{-1} acetonitrile solution of **4** at room temperature (full line), and absorption spectral changes on 365 nm irradiation of the same solution for 1, 3, 6, 12, and 25 min (dashed lines). The latter spectrum corresponds to the photostationary state. (Inset) Absorption spectrum of the **c** units in the photoproduct (dotted line) obtained by subtraction of the spectrum of the **tt** isomer (full line) from that of the photostationary state.

maximum at the PSS has decreased by no more than 50%, suggesting that only one-half of the available **t** photoresponsive units has isomerized. The presence of a set of clean isosbestic points at 325 and 464 nm indicates two possible scenarios for the photoreaction: (i) only two species coexist during the irradiation, namely, the **tt** and the **tc** forms, and nearly 100% of the **tc** isomer is obtained at the PSS or (ii) the three species coexist but in this case the spectra of the **tt**, **tc**, and **cc** forms must be simply given by a linear combination of the spectra of isolated photoactive units in their **t** or **c** forms. The absorption spectrum obtained by qualitative subtraction of the spectrum of the reactant from that of PSS is shown in the inset of Figure 2. This spectrum, which can be formally attributed to the **c** units in the photoproduct, shows two peaks at wavelengths longer than 300 nm, namely, centered at 347 and 466 nm. As will be shown in the next sections, the computational results on the structure, stability, excitation energies, and intensities of the three geometric isomers of **4** are more consistent with hypothesis i of coexistence of two (**tt** and **tc**) of the three species at the PSS.

3.2. Conformers, Ground-State Structures, and $\pi-\pi^*$ Excitations of the tt Geometric Isomer of 4. The azobenzenophane **4** forms a ring composed by 16 atoms and bonds. The CC and CN single bonds confer some flexibility to the macrocycle, although previously investigated azobenzenophanes were characterized by larger rings (compound **2**[12,13]) or a greater number of single bonds (compound **1**[11]), with a resulting reduced stiffness compared to **4**. The presence of single bonds in the macrocycle may result in the availability of several conformations for a given geometric isomer, arising from rotation around the CC or CN single bonds. Thus, before discussing the photoisomerization reaction of **4**, we wish to briefly consider the conformations that might contribute to the population of the initially prepared **tt** geometric isomer of **4**, subject to irradiation. Whereas a complete conformation search may provide the full ensemble of possible conformations, the following simple considerations restrict the investigation to a small number of conformers, relevant for the purpose of this study. First, we can consider that the **tt** geometric isomer of **4** can be built by accommodating the two **t** photoresponsive units in the three different configurations labeled **tt1**, **tt2**, and **tt3** in Chart 2. In the schematic representations of Chart 2, configurations **tt1** and **tt3** have the two azobenzene units with their NN double bonds oriented parallel to each other. However, in configuration **tt1** the CN_aN_b vertexes point inside the macrocycle, whereas in **tt3** they point outside. Finally, in configuration **tt2** the two NN bonds are not parallel. In addition to the reciprocal position of the two NN double bonds, the $-CH_2-$ bridges can point on the same side (up, up (**uu**)), as indicated in Chart 2, or on opposite sides (up, down (**ud**)). Thus, we may expect that the lowest energy structures of the **tt** geometric isomer will be found among the **tt1(uu)**, **tt1(ud)**, **tt2(uu)**, **tt2-(ud)**, **tt3(uu)**, and **tt3(ud)** conformations. Starting from the **tt1-(uu)** conformer, we found the energies and structures of the remaining two **uu** and the three **ud** conformers with a partial conformational search carried out with Tinker.[19] The energies of the structures investigated are collected in Table 2. Most of the structures found with the molecular mechanics calculations were re-optimized at the ab initio HF/3-21G level. Both MM3 and ab initio calculations predict the same lowest energy structure, namely, the **tt1(uu)** conformer, followed by the **tt1-(ud)** conformer which is computed to be 4.5 kcal/mol (5.8 kcal/mol from HF/3-21G calculations) less stable. A graphical representation of the HF/3-21G-optimized structures of the **tt** conformers of **4** is presented in Figures 3 and 4, along with the most relevant computed geometrical parameters. The CN and NN bond lengths of the two photoresponsive units in the macrocycle are similar to those computed for **3** and summarized in Figure 5. In particular, the CN bond connected to the *para*-aminobenzene (1.415 Å in **3**) is slightly shorter than the CN bond connected to the unsubstituted phenyl (1.427 Å in **3**), owing to the influence of tautomeric species. Inspection of the three dihedral angles in the region of the NN bond, indicated in Figures 3 and 4, shows that the nonplanarity of the chromophore increases for **uu** conformers in the same order as

CHART 2: Possible Conformers of the tt Geometrical Isomer of 4

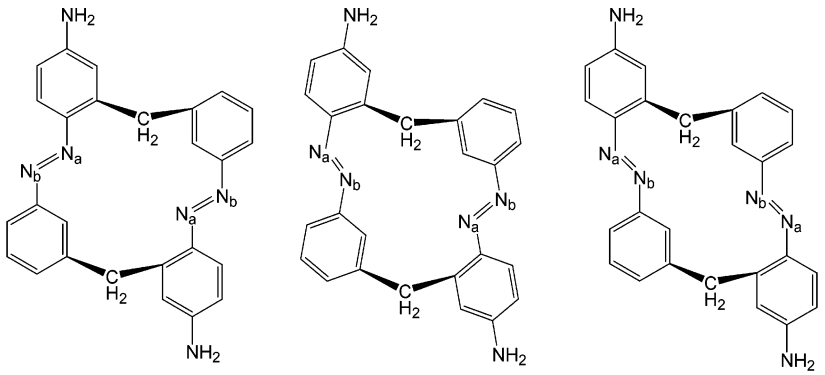

tt1(uu) **tt2(uu)** **tt3(uu)**

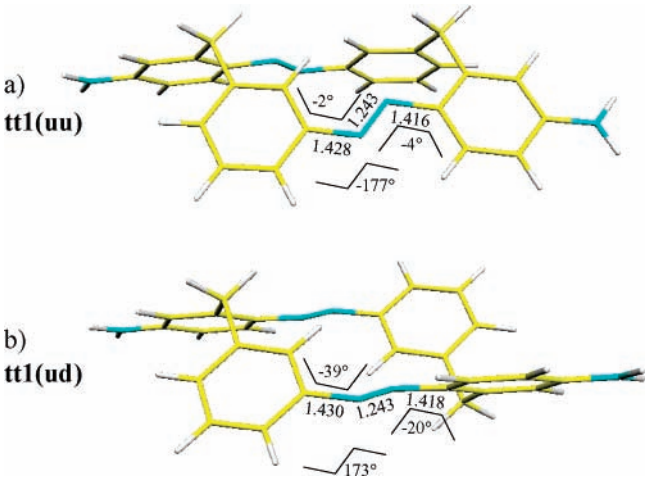

Figure 3. HF/3-21G equilibrium structures of the ground state of the (a) **tt1(uu)** and (b) **tt1(ud)** conformers of the **tt** geometric isomer of **4**.

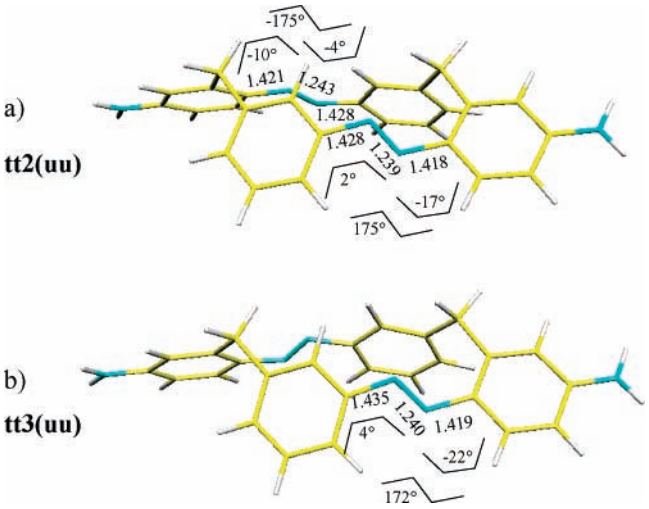

Figure 4. HF/3-21G equilibrium structures of the ground state of the (a) **tt2(uu)** and (b) **tt3(uu)** conformers of the **tt** geometric isomer of **4**.

their relative energy, namely, **tt3(uu)** > **tt2(uu)** > **tt1(uu)**. To assess the quality of the predicted energy differences for the various conformers of the **tt** geometric isomer, we can compare the HF/3-21G (19.6 kcal/mol) and MM3 (15.5 kcal/mol) energy differences between the **t** and **c** forms of azobenzene with the experimental value of about 10−12 kcal/mol.[27,28] Considering the computed overestimate by both methods, we can extrapolate a lower limit of ca. 3.0 kcal/mol for the energy difference between the **tt1(uu)** and the **tt1(ud)** forms. Under the above assumption, for an equilibrated sample at 298 K, the ratio between the populations of the two lowest energy forms is ca. 5×10^{-3}. Thus, the contribution of the **tt1(ud)** form, namely, the second lowest energy **tt** conformer, can be considered negligible, and this will hold even more strictly for the population of the remaining higher energy conformers.

Although such energy considerations underscore the negligible relevance of conformations different from the **tt1(uu)**, we can gain further support to the above conclusion by considering the spectroscopic properties predicted for the various **tt** conformers. To this end we evaluated ZINDO/S vertical excitations energies and intensities for all the HF/3-21G-optimized **tt** structures. The lowest $\pi-\pi^*$ transition energies are collected in the last column of Table 2. As expected, two close $\pi-\pi^*$ transitions fall in the energy region with $\lambda > 300$ nm, owing to the presence of the two photoresponsive units in the macrocycle.

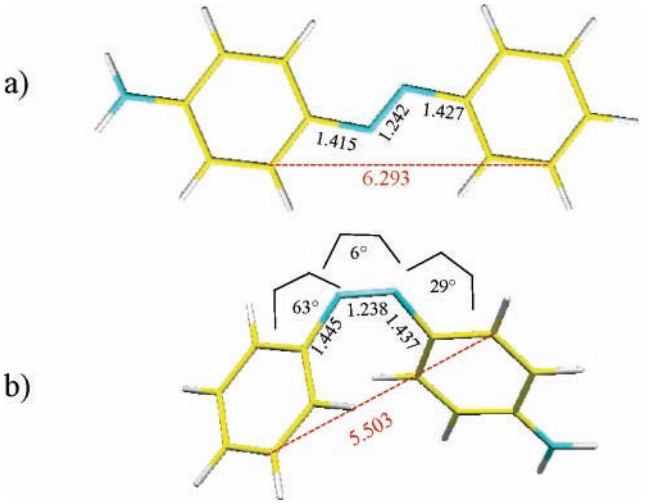

Figure 5. HF/3-21G equilibrium structure and selected intramolecular distances of the **t** and **c** isomers of **3**.

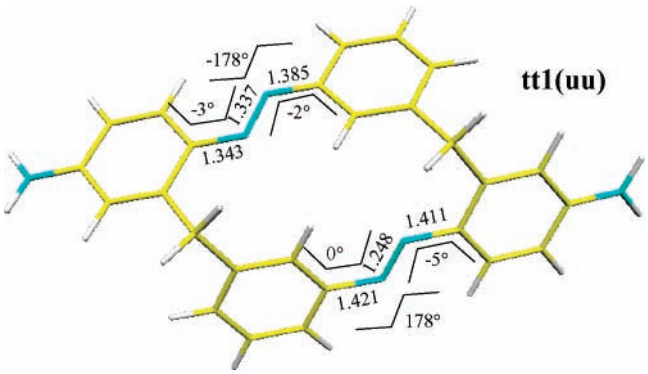

Figure 6. CIS/3-21G equilibrium structure of the lowest $\pi\pi^*$ state of the **tt1(uu)** conformer of the **tt** geometric isomer of **4**.

These are one-exciton delocalized states resulting from combinations of the lowest $\pi-\pi^*$ state of each azobenzene unit. It is interesting to note that for the **tt** isomers of **4** the total computed intensity for the two $\pi-\pi^*$ transitions is lower than twice the intensity of the $\pi-\pi^*$ transition of **3,** in agreement with the experimental data (Table 1). Such intensity decrease can be rationalized by considering that the transition dipole moments associated with the $\pi-\pi^*$ states localized on the azobenzene units do not lie in the same plane. Generally, the lowest of the two $\pi-\pi^*$ transitions is predicted to be dipole forbidden; thus, only the second one is relevant for comparison with the experimental absorption data. As pointed out in the previous subsection, the experimental absorption spectrum of the **tt** form of **4** is similar to that of the **t** isomer of **3**. By keeping in mind the slight overestimate in the ZINDO/S-predicted $\pi-\pi^*$ transition energies for **3**, we notice that the best agreement is found for the most stable **tt1(uu)** conformer, whose $\pi-\pi^*$ transition energy is computed at 366 nm, that is, identical to that of the **t** isomer of **3**. Note that the $\pi-\pi^*$ transition energy computed for the remaining **uu** conformers is slightly blue shifted, while it is remarkably blue shifted for the second lowest energy **tt1(ud)** conformer. We can conclude that the predominance of the **tt1(uu)** form is supported also by the excitation energy calculations.

3.3. tt → tc → cc Photoreaction and Structure of tc and cc Geometric Isomers. The photoisomerization mechanism of azobenzene has been discussed in several papers, and it has been recently shown, by high level quantum-chemical calculations, that the torsional path is preferred not only in the $\pi-\pi^*$

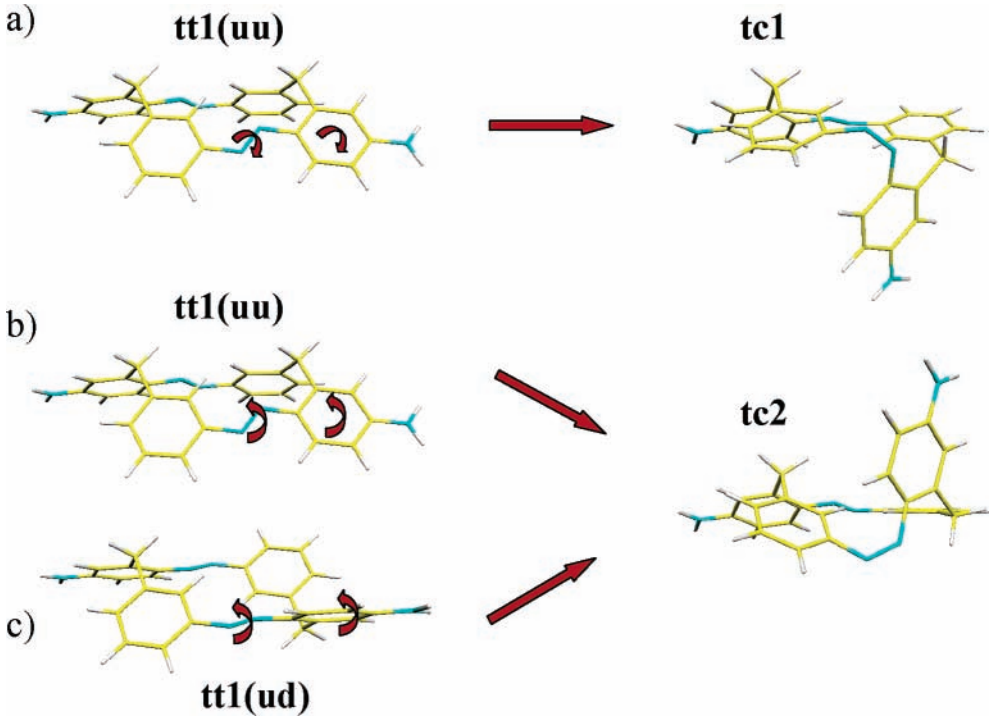

Figure 7. Possible photoisomerization paths for the **tt1(uu)** and **tt1(ud)** isomers and final **tc** photoproducts.

state but also in the lowest n−π* state.[29,30] Upon irradiation in the $\pi-\pi$* region of the dominant **tt1(uu)** conformer of **4**, one or both the photoresponsive units could in principle isomerize. The large dimension of the macrocycle investigated in this work prevents the use of the high-level calculations employed in recent azobenzene studies.[29] For this reason here we restrict the discussion to a more qualitative level with an approach that was used successfully in a recent investigation on bis(azo) derivatives[31] to provide a convincing explanation for their different photoisomerization behavior and efficiency. First, we wish to discriminate between the two possible isomerization routes, namely, (i) the sequential photoisomerization of a single NN bond or (ii) the simultaneous isomerization of both photoresponsive units in the macrocycle. Because the torsional path will correspond, at least initially, to the preferred deactivation channel also for compound **4**, to identify the most favorable route i or ii above we can inspect, with CIS/3-21G ab initio calculations, the relaxed excited-state geometry in the lowest $\pi-\pi$* state of the **tt1(uu)** conformer of **4**. The most relevant geometrical parameters are collected in Figure 6. The lowest energy $\pi-\pi$* state of **tt1(uu)** relaxes to a localized structure characterized by two NN bond lengths remarkably different, and the molecule loses the C_2 symmetry axis. One NN remains virtually unchanged, and the other increases to 1.337 Å. The remarkable elongation of a single NN bond, the torsion of which will be highly facilitated, supports, on one side, the similar photoisomerization efficiency of **4** and **3** and, on the other side, the hypothesis i of a sequential **tt** → **tc** → **cc** photoisomerization mechanism rather than the simultaneous photoisomerization of the two NN bonds. A similar behavior was observed and predicted for bis(azo) compounds constituted of a pair of azobenzene units sharing one of their phenyl rings with the two azo groups connected meta to the central phenyl.[31] The presence of a localized relaxed structure for compound **4**, similarly to the bis(azo) compound mentioned above, can be ascribed to the efficiency of the electron−phonon coupling mediated by the asymmetric NN stretching vibrational mode, characterized by elongation of one NN bond and shortening of the other NN bond. This interaction drives the localization of the excitation in the lowest $\pi-\pi$* state by coupling and mixing the close pair of $\pi-\pi$* one-exciton delocalized states.

Having established that the first photoisomerization reaction involves only one of the two photoresponsive units in the macrocycle, we explored the structure of the more plausible **tc** isomer. Owing to the limited flexibility of the azobenzenophane, the most natural, lowest energy path for **t** → **c** photoreaction involves the motion of the *para*-aminobenzene toward the interior of the basin formed by the macrocycle, as shown in Figure 7a. The correspondingly HF/3-21G-optimized structure of the **tc** isomer, labeled **tc1**, is shown in Figure 8a. Owing to ring strain, the two photoresponsive units, along with the two CH_2 bridges, are subject to some distortion in the **tc1** isomer. Indeed, the **t** unit is not planar, and the dihedrals around the CN bonds in the **c** unit are markedly larger than in the **c** form of **3**. Nevertheless, readjustment of the dihedral angles leaves the two intramolecular distances of **4**, indicated in red in the figure, very similar to those computed for **3** (see Figure 5). The effect of strain is reflected in the larger energy difference between **tc1** and **tt1(uu)** (25.0 kcal/mol), compared with the predicted **c**−**t** energy difference of **3** which is only 20.1 kcal/mol at the same level of theory. Note that the higher energy of the **tc1** isomer is associated with a reduction of the energy barrier for the thermal back reaction. Indeed, the HF/3-21G-computed ground-state energy barrier along the **tc1** → **tt1(uu)** path is 24.7 kca/mol, compared to ca. 29 kcal/mol computed for the **c** → **t** torsional path in **3**. Because of the moderate level of theory employed, the computed energy barriers are overestimated. Nevertheless, the significant reduction for **4** is in agreement with the observation of a faster backward reaction of the azobenzenophane with respect to **3** (see section 3.1 and Table 1).

Similarly to the **tt** isomer discussed in the previous section, several conformers corresponding to the **tc** geometric isomer may exist. MM3 conformational analysis calculations have indeed generated an additional **tc** isomer (labeled **tc2**) 0.6 kcal/mol more stable than the **tc1** structure. HF/3-21G optimization of the MM3 structure leads to a more remarkable energy

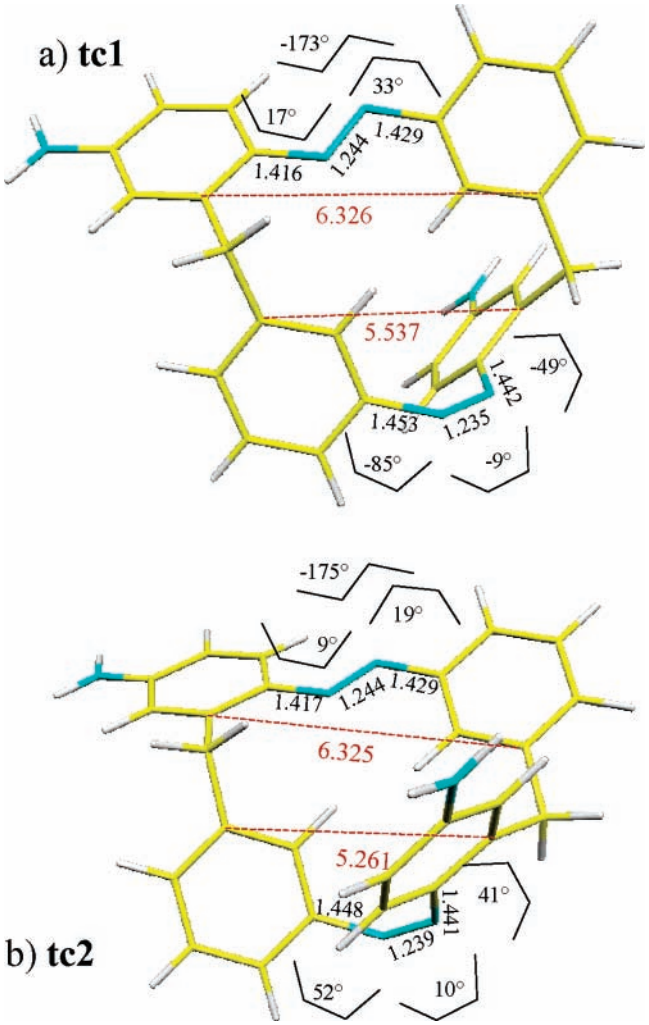

Figure 8. HF/3-21G equilibrium structure and selected intramolecular distances of the **tc1** and **tc2** isomers of **4.**

stabilization of 4.4 kcal/mol. The corresponding structure is shown in Figure 8b. Inspection of the selected dihedral angles indicated in the figure shows that the **tc2** isomer is characterized by a slightly reduced strain, compared to **tc1**, which justifies its lower energy. In contrast with **tc1**, formation of the **tc2** structure from **tt1(uu)**, as shown in Figure 7b, involves the motion of the *para*-aminobenzene toward the exterior of the basin formed by the macrocycle, with a concomitant partial inversion of the CH_2 bridge. Inversion of the CH_2 bridge will be associated with an energy barrier not only in the ground state but also in the excited state, and for this reason we deem highly unlikely that the **tt** → **tc** photoisomerization of **tt1(uu)** will proceed through path b in Figure 7. Conversely, formation of the **tc2** conformer seems more likely for the **tt** → **tc** photoisomerization of **tt1(ud)**, as shown in Figure 7c, although its contribution to the formation of the photoproduct will be negligible owing to the negligible population of the **tt1(ud)** conformer in the initially prepared compound **4**. Thus, in summary, the calculations indicate that the **tc** component of the photoproduct will be dominated by the **tc1** conformer. In passing we note that, as expected, the constrain introduced by the macrocycle induces an asymmetry in the potential energy surface describing the **t** → **c** photoisomerization of each azobenzene unit, thereby favoring the twisting of the dominant conformer **tt1(uu)** in one direction, namely, along path a in Figure 7, rather than in the other direction, along path b.

It can be expected that prolonged irradiation at 365 nm of the PSS of **4**, which must contain at least some amount of the **tc** forms (see Figure 2), leads to further isomerization of the second azobenzene unit in the macrocycle to form the **cc** species. In support of this, CIS/3-21G calculations of structure relaxation in the lowest $\pi-\pi^*$ state of the **tc1** species indicate a localized elongation of the NN bond of the **t** unit. In line with the discussion concerning the first step of the photoreaction, we considered two possible structures for the final **cc** product, corresponding to (i) isomerization of the **t** azobenzene unit in **tc1** by twisting the *para*-aminobenzene inside the basin formed by the macrocycle, namely, path a in Figure 9, leading to the final **cc1** isomer and (ii) twisting the *para*-aminobenzene outside the basin formed by the macrocycle, along path b in Figure 9, leading to the **cc2** isomer. Path b can be considered less probable than path a because the isomerization along this route is associated with the energetically unfavorable partial inversion of the CH_2 group, as for path b in Figure 7. Thus, the second isomerization step is expected to occur mainly along path a in Figure 9, leading to the **cc1** conformer, whose energy is predicted to be lower than that of the **cc2** isomer both by molecular mechanics and by ab initio calculations (see Table 2). The HF/3-21G-optimized structures of the **cc1** and **cc2** conformers are shown in Figure 10. An interesting feature of the **cc1** structure is the proximity of the two NH_2 substituents, which favors formation of hydrogen bonding, as indicated in the figure, thereby stabilizing this conformer with respect to **cc2**.

The possible reasons for the lack of accumulation of the **cc** form, as shown by the photochemical experiments, will be discussed in the next section.

4. Discussion

The results presented in the previous sections point to a stepwise photoisomerization of the macrocycle with the first step leading to a **tc** structure. The calculations also indicate that the energy and intensity of the lowest $\pi-\pi^*$ transitions dominantly localized on the **t** and **c** units (Table 2) do depend on the isomeric form of the neighboring azobenzene unit in the macrocycle, as expected for a structurally constrained molecule like **4**. Since clean isosbestic points are observed in the absorption spectra on irradiation of **4** at the wavelength of maximum absorption of the **tt** form, it is reasonable to conclude that only two compounds are present in the irradiated mixture, namely, the **tt** and **tc** isomers. Therefore, the absorption spectrum at the PSS is dominated by that of the **tc** isomer (or more precisely, according to the calculations, by the **tc1** structure) because nearly 50% of the **t** units have isomerized. This hypothesis is also supported by the fact that the absorption spectrum at the PSS reverts to the original spectrum (**tt** form) according to a single first-order process, whose rate constant is faster than that of the corresponding process of **3**, in line with the lower energy barrier computed for the **tc1** → **tt1(uu)** process compared with that of the **c** → **t** thermal reaction of **3**. Thus, from a spectroscopic point of view, we can identify the maximum observed at 388 nm in the PSS spectrum with the $\pi-\pi^*$ peak due to the **tc** form. We calculated the ZINDO/S vertical excitation energies of the lowest $\pi-\pi^*$ states for both the **tc1** and **tc2** structures. The calculations, summarized in the last column of Table 2, show a similar trend for the two structures. The **tc1** isomer is characterized by a lowest energy $\pi-\pi^*$ transition at 361 nm, carrying most of the intensity, and by a second, less intense, $\pi-\pi^*$ transition at 332 nm, while the **tc2** isomer is characterized by two $\pi-\pi^*$ transitions of

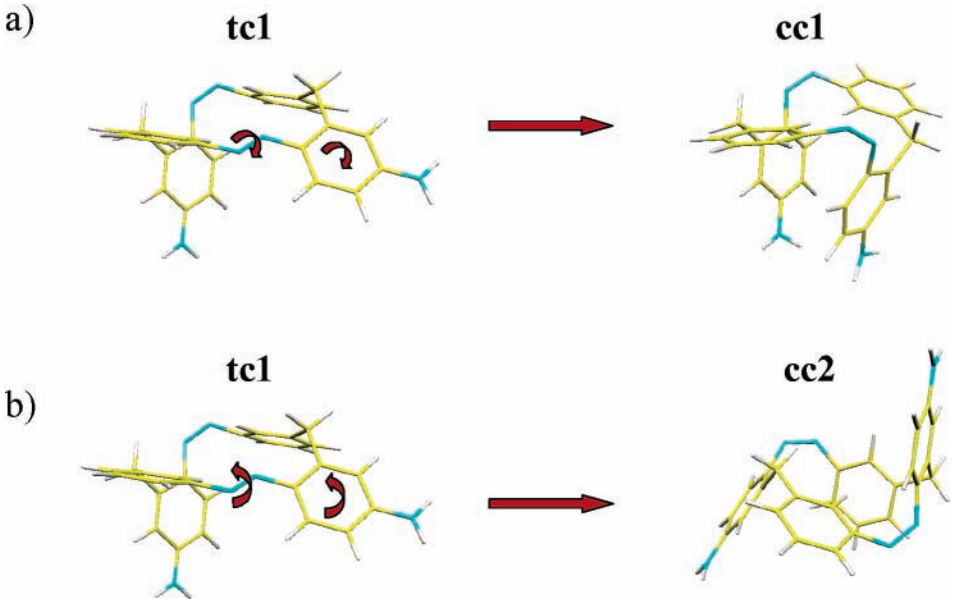

Figure 9. Possible photoisomerization paths for the **tc1** isomer and final **cc** photoproducts.

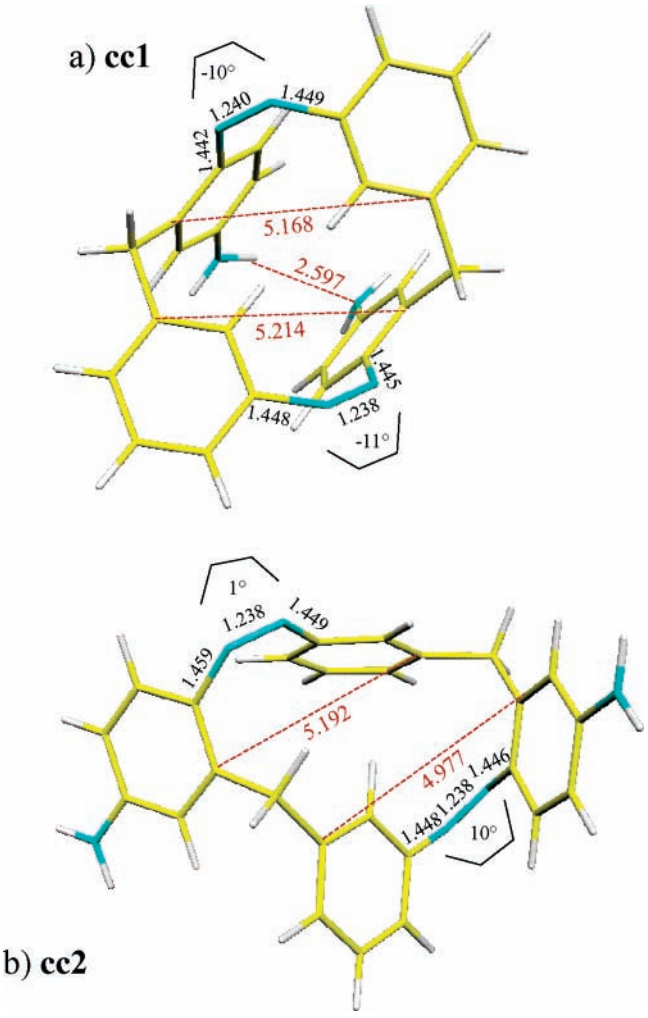

Figure 10. HF/3-21G equilibrium structure and selected intramolecular distances of the **cc1** and **cc2** isomers of **4.**

similar intensity at 372 and 347 nm. In other words, for both species the predicted spectrum indicates a minor blue shift of the overall $\pi-\pi^*$ peak, with respect to the spectrum computed for the **tt1(uu)** form, featuring an intense band at 366 nm. These changes match closely those observed between the initial spectrum of **4** and that of the PSS and add support to the conclusion that the PSS state is dominated by the **tc** form, although the low resolution of the spectrum prevents a more precise spectroscopic identification of the **tc1** or **tc2** species. The minor difference between the spectra computed for the **tc1** and **tc2** structures underscores the minor electronic communication and excitonic coupling that characterizes these compounds.

Noteworthy, the **tt** → **tc** conversion for macrocycle **4** at the PSS is nearly 100%, that is, larger than the **t** → **c** conversion observed for **3** in the same conditions. Considering that the quantum yield for the **t** → **c** isomerization of the (first) azobenzene unit is similar in **3** and **4** and that the thermal **c** → **t** isomerization for **4** is faster than that for **3**, it seems reasonable to suggest that the **tc** → **tt** quantum yield is smaller than the **t** → **c** quantum yield for **3**. However, the filtering effect exerted by the **t** units toward the **c** units in the **tc** form of **4** at the irradiation wavelength should also be considered. Further speculations would be unsafe on the basis of our results.

The observation of the second step of photoisomerization of **4** is hampered by the fast thermal **tc** → **tt** back reaction of the **tc** isomer. If it occurred, however, one would expect a slower **cc** → **tc** back reaction, as suggested by the computed energy barrier for the **cc1** → **tc1** thermal isomerization, which is 28 kcal/mol, that is ca. 3.3 kcal/mol higher than that for the **tc1** → **tt1(uu)** isomerization. The barrier for **cc1** → **tc1** reaction increases also because of the relative stability of the **cc1** isomer with respect to **tc1**. Indeed, the computed energy difference between the **tc1** and **cc1** forms of **4** is only 15.7 kcal/mol, compared to 20.1 kcal/mol for the **c**−**t** energy difference of **3**. The reduced energy difference is mainly due to the large energy of the highly strained **tc1** form, which reduces the gap with the **cc1** isomer. The energy of the latter is computed to be 40.7 kcal/mol above that of the **tt1(uu)** form, which is about twice the **c**−**t** energy difference computed for **3**. This does not imply that strain is totally absent in **cc1** but rather that it is compensated by the formation of the hydrogen bond. In conclusion, if a substantial fraction of the photoproduct had reached the **cc** form, we would expect an overall back reaction rate similar to that of compound **3**. Conversely, the observation of a thermal reaction which obeys first-order kinetics and is twice as fast for **4** compared to **3** is compatible with formation of the sole **tc** form. We can however attempt to compare the difference spectrum

show in the inset of Figure 2 (see section 3.1) obtained by subtracting the initial spectrum of **4** from that of the PSS with the computed spectroscopic data for the **cc1** and **cc2** species. The significance of the difference spectrum in the case of compound **4** should be taken with caution since the procedure to obtain it assumes implicitly that the **t** units absorb at exactly the same wavelength for the **tt** and **tc** species. As indicated by the calculations, this is only approximately true for **4**. Under the above assumptions, the difference spectrum represents the absorption due to the **c** units of the **tc** and **cc** isomers possibly contributing to the PSS.

The difference spectrum shows a peak approximately in the same region (ca. 347 nm) of the **c** form of **3**, although slightly red shifted. The ZINDO/S-computed **c** peak of **tc1** (see Table 2) is blue shifted by a slight amount (332 nm) compared to **c** form of **3** (337 nm). The computed peaks of **cc1** (or **cc2**) are red shifted by a larger amount (for **cc1** two peaks at 341 and 351 nm with similar intensities, that is an average peak at ca. 346 nm and one peak at ca. 354 nm for **cc2**). The minor change in the peak position computed for the **tc1** form, rather than the larger shift predicted for the **cc** forms, taken with due caution, seems in better agreement with the experiment.

The lack of accumulation of the **cc** form upon prolonged irradiation of the PSS, despite its predicted longer lifetime, points to a reduced photoreactivity of the **t** azobenzene units in the **tc1** isomer and/or to a high quantum yield for the **cc** → **tc** process. It is reasonable to propose that the photoreactivity of the azo units will be dependent on the isomeric form of the cyclophane (**tt**, **tc**, or **cc**) and on its conformational freedom. A detailed investigation on this aspect would require more thorough photochemical experiments together with computational studies of the excited-state properties and reactivity, which are beyond the scope of this work.

5. Concluding Remarks

The photoisomerization properties of *para*-aminoazobenzene **3** and azobenzenophane **4** have been studied by a combination of experimental and computational investigations. Both **3** and **4** undergo photoisomerization with similar quantum yields upon irradiation at 365 nm. Whereas the **t** → **c** photoconversion of **3** is close to 80%, that of **4** is only 50%. The backward thermal reaction is faster than that of azobenzene, and it is twice as fast for **4** compared to **3**.

Compound **4** is a macrocycle formed by 16 atoms, as the previously investigated [2.2](2,2′)-azobenzenophane,[11] but it contains a reduced number of single bonds. As a result it is considerably more stiff and strained than previously investigated cyclic azo compounds. Six possible conformers of the **tt** geometric isomer have been identified by means of molecular mechanics and ab initio calculations, and it has been shown that only the lowest energy conformer **tt1(uu)** dominates the population of the **tt** form of **4**.

A localized structure has been computed for the relaxed geometry of the lowest $\pi-\pi^*$ excited state of the **tt1(uu)** isomer, indicating the presence of a relatively strong electron−phonon coupling mediated through the asymmetric NN stretching vibration, which overcomes the exciton delocalization and splitting of the lowest two $\pi-\pi^*$ states of the macrocycle. As a result, a preference for a sequential **tt** → **tc** → **cc** photoisomerization reaction is suggested.

The most probable photoisomerization path has been identified by ab initio calculations for **tt1(uu)** along with the structure and energy of the **tc1** photoproduct. Similarly, the most probable path and photoproduct **cc1** for the second step (**tc** → **cc**) of the photoisomerization reaction have been identified.

The presence of the amino groups in para position, responsible for the faster back reaction of both **3** and **4** compared to azobenzene, along with the remarkable strain of the **tc1** photoproduct of **4** account for the fast thermal backward rate of **4**. The occurrence of such a process is indeed one of the reasons for the low photoconversion of **4**. Although computations suggest that the strain in the **cc** form would be counterbalanced by formation of a stabilizing intramolecular hydrogen bond between the two amino groups, the **cc** form cannot be obtained in an appreciable amount on irradiation of the **tc1** isomer. It is suggested that the conformational constraints of macrocycle **4** can affect the excited-state reactivity of its constituting azobenzene units.

Molecules such as **4**, owing to the macrocyclic structure, conformational properties, and full reversibility of the isomerization reaction, are promising candidates for construction of light-controlled switches[32] and development of photoelastic devices.[33,34]

Acknowledgment. This work was supported by funds from MURST PRIN 2004 (project: Spettroscopia rotazionale in assorbimento e a trasformate di Fourier: Produzione e studio di nuovi cluster e specie molecolari in espansioni supersoniche), MURST PRIN 2005 (project: Modellazione e caratterizzazione di cristalli liquidi per strutture nano-organizzate), MURST PRIN 2005 (project: Trasferimenti di energia e di carica a livello molecolare), and FIRB 2001 (project: "Carbon based micro and nanostructures", RBNE019NKS). A.C. acknowledges support from the Ministero degli Affari Esteri, Direzione Generale per la Promozione e la Cooperazione Culturale.

References and Notes

(1) Rau, H. In *Photochromism: Molecules and Systems*; Dürr, H., Bouas-Laurent, H., Eds.; Elsevier: Amsterdam, 2003; pp 165−92.
(2) Murakami, H.; Kawabuchi, A.; Matsumoto, R.; Ido, T.; Nakashima, N. *J. Am. Chem. Soc.* **2005**, *127*, 15891−9.
(3) Hugel, T.; Holland, N. B.; Cattani, A.; Moroder, L.; Seitz, M.; Gaub, H. E. *Science* **2002**, *296*, 1103−6.
(4) Norikane, Y.; Tamaoki, N. *Org. Lett.* **2004**, *6*, 2595−8.
(5) Nagamani, S. A.; Norikane, Y.; Tamaoki, N. *J. Org. Chem.* **2005**, *70*, 9304−13.
(6) Jousselme, B.; Blanchard, P.; Gallego-Planas, N.; Delaunay, J.; Allain, M.; Richomme, P.; Levillain, E.; Roncali, J. *J. Am. Chem. Soc.* **2003**, *125*, 2888−9.
(7) Qu, D. H.; Wang, Q. C.; Ma, X.; Tian, H. *Chem.−Eur. J.* **2005**, *11*, 5929−37.
(8) Rau, H.; Lueddecke, E. *J. Am. Chem. Soc.* **1982**, *104*, 1616−20.
(9) Tamaoki, N.; Ogata, K.; Koseki, K.; Yamaoka, T. *Tetrahedron* **1990**, *46*, 5931−42.
(10) Tamaoki, N.; Koseki, K.; Yamaoka, T. *Angew. Chem., Int. Ed. Engl.* **1990**, *29*, 105−6.
(11) Tauer, E.; Machinek, R. *Liebigs Ann.* **1996**, 1213−6.
(12) Norikane, Y.; Kitamoto, K.; Tamaoki, N. *Org. Lett.* **2002**, *4*, 3907−10.
(13) Norikane, Y.; Kitamoto, K.; Tamaoki, N. *J. Org. Chem.* **2003**, *68*, 8291−304.
(14) Pieraccini, S.; Gottarelli, G.; Labruto, R.; Masiero, S.; Pandoli, O.; Spada, G. P. *Chem.−Eur. J.* **2004**, *10*, 5632−9.
(15) Hatchard, C. G.; Parker, C. A. *Proc. R. Soc. London* **1956**, *253*, 518.
(16) Fischer, E. *EPA Newsletter* **1984**, *20*, 33.
(17) Montalti, M.; Credi, A.; Prodi, L.; Gandolfi, M. T. *Handbook of Photochemistry*, 3rd ed.; CRC Press: Boca Raton, 2006.
(18) Allinger, N. L.; Yuh, H. Y.; Lii, J. H. *J. Am. Chem. Soc.* **1989**, *111*, 8551−66.
(19) Ponder, J. W. *TINKER, Software Tools for Molecular Design*, version 3.8 (1990−2003); http://dasher.wustl.edu/tinker.
(20) Bacon, A. D.; Zerner, M. C. *Theor. Chim. Acta* **1979**, *53*, 21.
(21) *Gaussian 03*, Revision B.1; Frisch, M. J.; Trucks, G. W.; Schlegel, H. B.; Scuseria, G. E.; Robb, M. A.; Cheeseman, J. R.; Montgomery, Jr.,

J. A.; Vreven, T.; Kudin, K. N.; Burant, J. C.; Millam, J. M.; Iyengar, S. S.; Tomasi, J.; Barone, V.; Mennucci, B.; Cossi, M.; Scalmani, G.; Rega, N.; Petersson, G. A.; Nakatsuji, H.; Hada, M.; Ehara, M.; Toyota, K.; Fukuda, R.; Hasegawa, J.; Ishida, M.; Nakajima, T.; Honda, Y.; Kitao, O.; Nakai, H.; Klene, M.; Li, X.; Knox, J. E.; Hratchian, H. P.; Cross, J. B.; Adamo, C.; Jaramillo, J.; Gomperts, R.; Stratmann, R. E.; Yazyev, O.; Austin, A. J.; Cammi, R.; Pomelli, C.; Ochterski, J. W.; Ayala, P. Y.; Morokuma, K.; Voth, G. A.; Salvador, P.; Dannenberg, J. J.; Zakrzewski, V. G.; Dapprich, S.; Daniels, A. D.; Strain, M. C.; Farkas, O.; Malick, D. K.; Rabuck, A. D.; Raghavachari, K.; Foresman, J. B.; Ortiz, J. V.; Cui, Q.; Baboul, A. G.; Clifford, S.; Cioslowski, J.; Stefanov, B. B.; Liu, G.; Liashenko, A.; Piskorz, P.; Komaromi, I.; Martin, R. L.; Fox, D. J.; Keith, T.; Al-Laham, M. A.; Peng, C. Y.; Nanayakkara, A.; Challacombe, M.; Gill, P. M. W.; Johnson, B.; Chen, W.; Wong, M. W.; Gonzalez, C.; Pople, J. A. Gaussian, Inc.: Pittsburgh, PA, 2003.

(22) *Molekel*, Version 4.3, http://www.cscs.ch/molekel/. Portmann, S.; Lüthi, H. P. *Chimia* **2000**, *54*, 766.

(23) Hirose, Y.; Yui, H.; Sawada, T. *J. Phys. Chem. A* **2002**, *106*, 3067−71.

(24) Halpern, J.; Brady, G. W.; Winkler, C. A. *Can. J. Res., Sect. B* **1950**, *28*, 140.

(25) Gabor, G.; Fischer, E. *J. Phys. Chem.* **1971**, *75*, 581−3.

(26) For the same reason, NMR determination of the composition of the PSS was unsuccessful. Experiments were run on 10^{-4} mol L^{-1} solutions previously subjected to exhaustive irradiation at 365 nm (at 25 °C). The ^{1}H NMR spectrum recorded at 25 and −20 °C revealed only the presence of the signals of the **tt** form: the signals of any other species possibly present, if any, are not distinguishable from the background noise in these experimental conditions.

(27) Adamson, A. W.; Vogler, A.; Kunkely, H.; Wachter, R. *J. Am. Chem. Soc.* **1978**, *100*, 1298−300.

(28) Corruccini, R. J.; Gilbert, E. C. *J. Am. Chem. Soc.* **1939**, *61*, 2925−7.

(29) Cembran, A.; Bernardi, F.; Garavelli, M.; Gagliardi, L.; Orlandi, G. *J. Am. Chem. Soc.* **2004**, *126*, 3234−43.

(30) Gagliardi, L.; Orlandi, G.; Bernardi, F.; Cembran, A.; Garavelli, M. *Theor. Chem. Acc.* **2004**, *111*, 363−72.

(31) Cisnetti, F.; Ballardini, R.; Credi, A.; Gandolfi, M. T.; Masiero, S.; Negri, F.; Pieraccini, S.; Spada, G. P. *Chem.—Eur. J.* **2004**, *10*, 2011−21.

(32) *Molecular Switches*; Feringa, B. L., Ed.; Wiley-WCH: Weinheim, 2001.

(33) Credi, A. *Aust. J. Chem.* **2006**, *59*, 157−69.

(34) Muraoka, T.; Kinbara, K.; Aida, T. *Nature* **2006**, *440*, 512−5.